Journal of Proteomics 131 (2016) 177–189

Contents lists available at ScienceDirect

Journal of Proteomics

journal homepage: www.elsevier.com/locate/jprot

Comparative proteomics of uropathogenic *Escherichia coli* during growth in human urine identify UCA-like (UCL) fimbriae as an adherence factor involved in biofilm formation and binding to uroepithelial cells

Daniël J. Wurpel [a], Makrina Totsika [b], Luke P. Allsopp [c], Richard I. Webb [d], Danilo G. Moriel [a], Mark A. Schembri [a,*]

[a] Australian Infectious Disease Research Centre, School of Chemistry and Molecular Biosciences, The University of Queensland, Brisbane, Australia
[b] Institute of Health and Biomedical Innovation, School of Biomedical Sciences, Queensland University of Technology, Brisbane, Australia
[c] MRC Centre for Molecular Bacteriology and Infection, Department of Life Sciences, Imperial College London, London, United Kingdom
[d] Centre for Microscopy and Microanalysis, The University of Queensland, Brisbane, Australia

ARTICLE INFO

Article history:
Received 1 July 2015
Received in revised form 23 October 2015
Accepted 2 November 2015
Available online 3 November 2015

Keywords:
F17-like
Chaperone-usher
Pili
Proteome
Outer membrane
Vesicles
UPEC
Adhesion

ABSTRACT

Uropathogenic *Escherichia coli* (UPEC) are the primary cause of urinary tract infection (UTI) in humans. For the successful colonisation of the human urinary tract, UPEC employ a diverse collection of secreted or surface-exposed virulence factors including toxins, iron acquisition systems and adhesins. In this study, a comparative proteomic approach was utilised to define the UPEC pan and core surface proteome following growth in pooled human urine. Identified proteins were investigated for subcellular origin, prevalence and homology to characterised virulence factors. Fourteen core surface proteins were identified, as well as eleven iron uptake receptor proteins and four distinct fimbrial types, including type 1, P, F1C/S and a previously uncharacterised fimbrial type, designated *UCA-like* (UCL) fimbriae in this study. These pathogenicity island (PAI)-associated fimbriae are related to UCA fimbriae of *Proteus mirabilis*, associated with UPEC and exclusively found in members of the *E. coli* B2 and D phylogroup. We further demonstrated that UCL fimbriae promote significant biofilm formation on abiotic surfaces and mediate specific attachment to exfoliated human uroepithelial cells. Combined, this study has defined the surface proteomic profiles and core surface proteome of UPEC during growth in human urine and identified a new type of fimbriae that may contribute to UTI.

1. Introduction

Urinary tract infections (UTIs) are among the most common bacterial infections affecting humans. These infections cause significant morbidity and mortality, with an estimated global incidence of approximately 150 million cases per year [1–3]. Symptomatic UTIs typically present as bladder infection (cystitis), but may also manifest as kidney infection (acute pyelonephritis) and lead to urosepsis. It is estimated that more than half of all women will experience at least one UTI episode in their lifetime and one in four will undergo a recurrent infection within six months [4]. Antibiotic therapy is the first choice of treatment and as a result UTIs represent the second predominant reason for antibiotic prescription worldwide. However, the rapid rise in the incidence of UTIs caused by multidrug resistant bacteria has highlighted an urgent need for the development of novel therapeutic strategies [5–7].

Uropathogenic *Escherichia coli* (UPEC) are the predominant etiological agents of UTI, accounting for more than 80% of community acquired and 50% of nosocomial infections [2,8]. Due to their role in pathogenesis, UPEC surface-exposed virulence factors represent attractive targets for the development of new diagnostic, drug and vaccine applications. As a result of the extensive genetic and phenotypic heterogeneity that exists between individual UPEC strains, however, the development of novel broadly protective therapeutic solutions to prevent UPEC-mediated UTI has been challenging [9]. Accordingly, a comparative analysis of the UPEC cell surface is paramount for the identification of ubiquitous surface antigens that can serve as common targets for treatment.

Genes encoding virulence factors are typically located on horizontally acquired mobile genomic elements called pathogenicity islands (PAIs) [10,11]. Although no single virulence gene is definitive for UPEC pathogenesis, a complementary array of factors including iron acquisition systems, toxins and adhesins facilitate bacterial colonisation and persistence within the human urinary tract. Adherence to uroepithelial cells is a critical initial step in uropathogenesis as it enables UPEC to resist the hydrodynamic forces of urine flow and promotes colonisation. In mice, UPEC adherence also leads to the invasion of superficial bladder

* Corresponding author at: School of Chemistry and Molecular Biosciences, Building 76, The University of Queensland, Brisbane QLD 4072, Australia.
E-mail address: m.schembri@uq.edu.au (M.A. Schembri).

http://dx.doi.org/10.1016/j.jprot.2015.11.001

epithelial cells and the subsequent formation of intracellular bacterial communities (IBCs) [12,13]. While UPEC possess a diverse array of adherence factors, fimbriae of the chaperone-usher (CU) secretion pathway such as type 1, P, F1C/S and AFA fimbriae represent the primary mediators for colonisation of the urinary tract [13–16]. Other factors that contribute to UPEC bladder colonisation include autotransporter adhesins and curli (for a review refer to [17]).

The CU pathway is a highly conserved secretion pathway in Gram-negative bacteria that facilitates the production of fimbriae. The biogenesis of CU fimbriae involves a dedicated periplasmic chaperone and an integral outer membrane (OM) usher protein, which functions as an assembly platform for the formation of the fimbrial heteropolymer [18,19]. The bulk of the fimbrial organelle consists of approximately 500 to 3000 major subunit monomers and typically contains a receptor-binding adhesin subunit at the distal tip [20]. The adhesin is composed of two distinct protein domains [18]; the C-terminal domain connects the adhesin to the main fimbrial shaft, sometimes aided by one or more minor subunits, while the N-terminal lectin domain mediates attachment to specific ligands, effectively determining the adhesive phenotype of the fimbriae [21]. The structural genes encoding CU fimbriae are almost invariably organised as polycistronic operons. Genomic analysis of the *E. coli* pan-genome has identified 38 distinct CU fimbrial types based on genomic locus position and usher phylogeny, and revealed that a single strain may contain up to 17 fimbrial operons [22].

Type 1 and P fimbriae play a key role in UPEC pathogenesis by mediating attachment to α-D-mannosylated proteins on the bladder epithelium and α-Gal(1–4)β-Gal receptor epitopes in the upper urinary tract, respectively [14,18,23]. Other CU fimbriae associated with UPEC include the AFA/Dr adhesins, involved in adherence to collagen IV in the interstitial compartments of the kidneys, and F1C/S fimbriae, which confer binding to GalNAcβ1-4Galβ glycolipids and sialyl galactoside glycoproteins, both present on epithelial cells lining the bladder and kidneys [15,24,25]. However, some UPEC strains are able to mediate attachment to uroepithelial cells in the absence of these well-characterised adhesins, indicating the existence of additional adherence factors involved in uropathogenesis [26].

In this study, we applied a method involving nanoscale liquid chromatography tandem mass spectrometry (nanoLC–MS/MS) of EDTA heat-induced outer membrane vesicles (OMVs) to characterise the surface proteome of five reference UPEC strains during *in vitro* growth in human urine. The analysis led to the identification of 173 unique proteins, which were characterised for subcellular origin, prevalence and homology to functionally characterised virulence factors. Of the predicted surface proteins identified, 14 were detected in all strains. Furthermore, we observed co-expression of up to nine distinct iron uptake systems in individual UPEC strains and four fimbrial types, including type 1, P, F1C/S and a previously uncharacterised fimbrial type, designated *UCA-like* (UCL) fimbriae in this work. We demonstrate that genes encoding UCL fimbriae are associated with UPEC strains and are phylogenetically related to UCA (Uroepithelial Cell Adhesin) fimbriae from *Proteus mirabilis* and F17/G fimbriae from *E. coli*. We also show that recombinant expression of these PAI-associated fimbriae mediates significant biofilm formation on abiotic surfaces and confer specific attachment to human exfoliated uroepithelial cells, suggesting a role in the colonisation of the human urinary tract.

2. Methods

2.1. Bacterial strains, plasmids and culture conditions

Strains and plasmids used in this study are listed in Table 1. Five reference UPEC strains whose genome sequence is available on the NCBI database were used: 536 [9], CFT073 [27], F11 [28], UMN026 [29] and UTI89 [30]. *E. coli* strains from a community acquired urosepsis collection [31] and from the *E. coli* Reference Collection (ECOR) [32] have been described previously. Strains were routinely cultured at 37 °C on solid or in liquid Lysogeny Broth (LB) medium [33] or liquid M9 glucose minimal medium (42 mM Na_2HPO_4, 22 mM KH_2PO_4, 9 mM NaCl, 18 mM NH_4Cl, 1 mM $MgSO_4$, 0.1 mM $CaCl_2$ and 0.2% (*w*/*v*) glucose). Where appropriate, media were supplemented with ampicillin (Amp, 100 μg ml^{-1}), kanamycin (Kan, 100 μg ml^{-1}) or chloramphenicol (Cam, 30 μg ml^{-1}). To induce expression of UCL fimbriae from plasmid pUCL, culture media were supplemented with 1 mM isopropyl β-D-1-thiogalactopyranoside (IPTG).

Table 1
Strains and plasmids used in this study.

E. coli strain or plasmid	Relevant characteristics	Reference
Strain		
536	Wild-type UPEC reference strain	Brzuszkiewicz et al. [9]
CFT073	Wild-type UPEC reference strain	Welch et al. [10]
F11	Wild-type UPEC reference strain	Rasko et al. [28]
UMN026	Wild-type UPEC reference strain	Touchon et al. [29]
UTI89	Wild-type UPEC reference strain	Chen et al. [30]
MS428	*E. coli* K-12 MG1655 *fim*	Kjaergaard et al. [47]
MS428(pSU2718)	pSU2718 in MS428, Cam^r	This study
MS428(pUCL)	pUCL in MS428, Cam^r	This study
MS428(pSU2718,pCO13)	pSU2718 and pCO13 in MS428, GFP^+ Kan^r Cam^r	This study
MS428(pUCL,pCO13)	pUCL and pCO13 in MS428, GFP^+ Kan^r Cam^r	This study
OS56	K-12 MG1655 *flu*, *attB*::*bla-gfp*, GFP^+ Amp^r	Sherlock et al. [75]
OS56(pSU2718)	pSU2718 in OS56, GFP^+ Amp^r Cam^r	This study
OS56(pUCL)	pUCL in OS56, GFP^+ Amp^r Cam^r	This study
Plasmid		
pSU2718	Cloning vector, Cam^r	Martinez et al. [76]
pUCL	ECP_3785–3782 (UCL_{536}) in pSU2718, Cam^r	This study
pCO13	*gfp* (GFP_{pKEN2}) containing plasmid, Kan^r	Ong et al. [77]

2.2. DNA manipulation and genetic techniques

Plasmid DNA was isolated using the QIAprep Spin Miniprep kit (Qiagen). Chromosomal DNA was purified using the GenomicPrep cell and tissue DNA isolation kit (GE Healthcare). General PCR reactions were performed using *Taq* DNA polymerase according to the manufacturer's instructions (Roche). For molecular cloning purposes, DNA was amplified using Phusion High-Fidelity DNA polymerase (Thermo Fisher Scientific). Oligonucleotide primers used in this study were purchased from Sigma-Aldrich and are listed in Table S1. The UCL fimbriae expression plasmid pUCL was constructed by Phusion High Fidelity PCR amplification of the entire 5 kb UCL gene cluster (ECP_3785–3782) from UPEC strain 536, using primers 3383 and 3384 containing 5′ XbaI and SphI restriction sites, respectively. The PCR product was then digested with XbaI and SphI and directionally cloned into the corresponding sites of cloning vector pSU2718, where expression of the *ucl* fimbrial operon on pUCL is controlled by the IPTG-inducible *lac* promoter. PCR products and plasmids were sequenced using the BigDye Terminator v3.1 cycle DNA sequencing kit according to the manufacturer's instructions (Life Technologies) at the Australian Equine Genome Research Centre. Plasmid transformations were mediated by electroporation.

2.3. Preparation of EDTA heat-induced outer membrane vesicles for mass spectrometric analysis

Bacterial strains were grown at 37 °C with shaking (250 rpm) to an optical density at 600 nm of approximately 0.8 in 50 ml of pooled, filter sterilised mid-stream urine (collected from 4 healthy female

volunteers). Preparation of OMVs was performed as previously described [31]. Briefly, cells were pelleted at 10,000 ×*g* for 10 min at 4 °C post-incubation and washed three times in 25 ml ice-cold sterile PBS. Bacteria were resuspended in 1 ml EDTA buffer (0.05 M Na_2HPO_4, 0.15 M NaCl, 0.01 M EDTA, pH 7.4) and incubated for 30 min at 56 °C. Cells were pelleted at 10,000 ×*g* for 10 min at 4 °C and the supernatant was collected and sterilised using a 0.22 μm PVDF low protein binding filter (Millipore). Proteins were precipitated by the addition of TCA to a final concentration of 20% (*w*/*v*) and incubated overnight at 4 °C, subsequently pelleted at 14,000 ×*g* for 30 min at 4 °C, washed 3 times in 1 ml 100% ethanol, briefly air-dried and dissolved at 60 °C in 50 μl resuspension buffer (50 mM ammonium bicarbonate, 3 M urea, 5 mM DTT). Proteins were alkylated for 30 min at room temperature in the dark using iodoacetamide (final concentration 22.5 μM) and afterwards diluted with 100 μl ammonium bicarbonate (50 mM). 50 μl protein sample was digested overnight at 37 °C by the addition of 5 μl sequencing grade modified trypsin (1 mg ml^{-1}, Promega).

2.4. Mass spectrometry and protein identification

Protein fractions were analysed by nanoLC–MS/MS as previously described [31]. Briefly, digested OMV samples (5 μl) were injected into a Prominence NanoLC (Shimadzu) coupled to a Triple TOF 5600 mass spectrometer (AB SCIEX) equipped with a nano-electrospray ion source, desalted for 5 min in a 50 mm × 300 μm C18 trap column (Agilent), and subsequently gradient-eluted using an in-line 150 mm × 75 μm C18 nanoLC column (Agilent). The mass spectrometer acquired 500 MS full scan TOF-MS data (mass range 350–1800) followed by 20 by 50 MS full scan product ion data in Information Dependant Acquisition (IDA) mode (mass range 100–1800). TOF-MS scan ions exceeding a 100 count threshold and a charge state of +2 to +5 were set to trigger product ion acquisition of the resultant 20 most intense ions. Spectral data were acquired and processed using Analyst TF 1.5.1 software (AB SCIEX), proteins were identified using the Paragon algorithm of the ProteinPilot v4.0.8085 Software Package (AB SCIEX) queried against the UniProt redundant *E. coli* proteome database [34]. Protein redundancy was investigated using an all-*vs*-all BLASTp query with a cut-off value of 75% of full-length sequence identity. BLASTp hits in the 65–75% identity range were investigated for shared locus synteny and classified accordingly. Protein sub-cellular location and signal-peptides/transmembrane domains were predicted with PSORTb v3.0.2 [35] and LipoP v1.0 [36], respectively. The Circos software package was used to generate a circular diagram of the proteomic data [37].

2.5. Multiple sequence alignment and phylogenetics

The MEGA5 software package was used to infer evolutionary relationships of UCL related fimbriae [38]. Full-length amino acid sequences of the UCL, UCA, F17/G and KTE194 (A13Y_00037–00040) fimbrial usher proteins were aligned by ClustalW using the BLOSUM protein weight matrix with default parameters. The evolutionary phylogeny of usher proteins was reconstructed with the Neighbour-Joining method, using the Jones–Taylor–Thornton (JTT) substitution model for the generation of distance matrices and a 1000 replicate bootstrap test of phylogeny. The resultant phylogenetic tree was visualised in iTOL [39]. Protein evolutionary divergence rates were estimated using the JTT correction model and standard error estimates were calculated using a bootstrap procedure of 1000 replicates. DNA sequences of the UCL, UCA, F17/G and KTE194 (A13Y_00037–00040) fimbrial operons and their corresponding genomic contexts were aligned and visualised in Easyfig 2.1 [40].

2.6. Electron microscopy

E. coli MS428 harbouring pUCL or pSU2718 (vector control) were cultured overnight in LB broth containing 1 mM IPTG and 30 μg ml^{-1} chloramphenicol at 37 °C, 250 rpm. Glow-discharged carbon-coated Formvar copper grids were placed on drops of bacterial suspension for 1 min and then washed on drops of water (3 × 1 min). Grids were negatively stained with 1% uranyl acetate and cells were examined under a JEOL 1010 TEM operated at 80 kV. Micrographs were captured using an analySIS Megaview III digital camera.

2.7. Biofilm assays

Bacterial biofilm formation was assessed on sterile non-coated 96-well polyvinyl chloride (PVC) microtitre plates (BD Falcon), essentially as previously described [41]. Cells were cultured in 150 μl M9 medium containing 1 mM IPTG and 30 μg ml^{-1} chloramphenicol for 24 h at 37 °C, 150 rpm. After incubation, cells were washed in dH_2O, stained with 0.1% crystal violet for 30 min at 4 °C, and washed three additional times. Bound bacterial cells were quantified by adding ethanol–acetone (80:20 *v*/*v*) and measurement of the dissolved crystal violet at an optical density of 595 nm.

Flow chamber biofilm assays were performed essentially as previously described [42]. Briefly, individual flow cells were inoculated with green fluorescent protein (GFP) tagged *E. coli* strain OS56 containing either plasmid pUCL or pSU2718 from a standardised (OD_{600} = 0.02) pre-culture and incubated at 28 °C in M9 medium containing 1 mM IPTG and 30 μg ml^{-1} chloramphenicol. Biofilms were allowed to form on glass coverslips (Menzel-Gläser) in a multichannel flow system at a flow rate of 4 ml/h that permitted monitoring of biofilm formation. Biofilm development was monitored at 24 h post-inoculation by confocal laser scanning microscopy (LSM 510 META, Zeiss), equipped with GFP specific filters and detectors. Biofilm cross-sections were visualised with the LSM Image Examiner software (Zeiss), 12 z-stacks were collected per strain for analysis in Matlab (Mathworks) using the COMSTAT software package [43].

2.8. Uroepithelial cell adherence assay

GFP expressing strains MS428(pSU2718,pCO13) and MS428 (pUCL,pCO13) were cultured overnight at 37 °C, 250 rpm in LB medium containing 1 mM IPTG, 30 μg ml^{-1} chloramphenicol, 100 μg ml^{-1} kanamycin and/or 100 μg ml^{-1} ampicillin where appropriate. Exfoliated uroepithelial cells were collected from pooled mid-stream urine from 4 healthy female donors by centrifugation at 500 ×*g* for 15 min and washed once in 25 ml PBS. 1×10^5 uroepithelial cells were resuspended in 1 ml PBS containing 1×10^9 bacterial cells (MOI: 10,000) and incubated for 30 min at 37 °C, 100 rpm. Cells were washed four times in 1 ml PBS and examined by epifluorescence/light microscopy (Axioplan 2, Zeiss). Bacterial adherence was assessed by counting the number of GFP-positive bacteria attached to 50 eukaryotic cells observed in randomly selected fields of view.

2.9. Statistical analyses

Peptide confidence intervals (CI) were calculated using the ProteinPilot Software v4.0.8085 scoring algorithm (AB SCIEX). Differences in UCL gene prevalence in *E. coli* isolates belonging to the ECOR and a urosepsis collection were determined using Fisher's exact test with a two-tailed *P* value. Bacterial biofilm formation in PVC microtitre plates was analysed using a two-tailed *t* test. COMSTAT data was analysed using the nonparametric Mann–Whitney Test within the Minitab (v.14) software package. *P* values < 0.05 were considered statistically significant.

2.10. Ethics statement

This study was performed in accordance with the ethical standards of the Helsinki Declaration. The study was approved and the need for informed consent was waived by the institutional review board of the Princess Alexandra Hospital (research protocol 2008/264).

Table 2
Proteins identified in EDTA heat-induced UPEC OMVs after growth in human urine

Accession	Protein	Description/annotation[a]	Functional classification[b]	LipoP[c]	Prevalence[d] (detected protein/gene)
Extracellular					
Q0T8Z4	FimA	Type-1 fimbriae major subunit	Adhesion	SpI	5/5
Q8GA68	UclA	F17-like fimbriae major subunit	Adhesion	SpI	2/3
Q8GA71	UclD	F17-like fimbriae adhesin subunit	Adhesion	SpI	1/3
Q8VR35	PapA	P fimbriae major subunit	Adhesion	SpI	3/5
Q93K75	SfaA	F1C/S fimbriae major subunit	Adhesion	SpI	4/4
Q9S0U1	FliC	Flagellin	Motility	CYT	4/5
D6IT07	SslE	Putative lipoprotein mucinase	Unknown	SpII	2/4
Q8FE01	HlyA	Hemolysin A	Cytotoxicity	CYT	3/4
Outer membrane					
Q14F40	BtuB	Vitamin B12 receptor	Transport	CYT	5/5
Q8CVW8	CirA	Colicin I sensitive receptor	Transport	CYT	4/5
Q9EZQ6	ChuA	Haem/haemoglobin receptor	Metal ion transport	SpI	5/5
Q933S4	CjrC	Putative siderophore receptor	Metal ion transport	SpI	3/3
Q8CWA1	FepA	Ferrienterobactin receptor	Metal ion transport	SpI	5/5
Q8X901	FhuA	Ferrichrome-iron receptor	Metal ion transport	SpI	2/5
B1LM97	Fiu	Catecholate siderophore receptor Fiu	Metal ion transport	SpI	4/5
Q9RQ18	FyuA	Yersiniabactin/pesticin receptor	Metal ion transport	SpI	5/5
Q8FDW0	IutA	Ferric aerobactin receptor	Metal ion transport	CYT	2/2
Q9LAP1	Iha	Siderophore receptor/adhesin	Metal ion transport	SpI	2/2
Q4FBD9	IreA	Putative siderophore receptor	Metal ion transport	SpI	1/1
Q93K73	IroN	Salmochelin receptor	Metal ion transport	SpI	4/4
Q1RAB2	UTI89_C2234	Putative iron compound receptor	Metal ion transport	SpI	3/4
C9QUX0	UidC	Outer membrane porin protein	Porin	SpI	5/5
Q8CVY9	NmpC	Outer membrane porin protein	Porin	CYT	5/5
Q1RDQ7	OmpA	Outer membrane protein A	Porin	SpI	5/5
D6JCB5	OmpC	Outer membrane protein C	Porin	SpI	5/5
Q8XDF1	OmpF	Outer membrane protein F	Porin	SpI	5/5
Q0TKA6	OmpT	Outer membrane protein T, protease VII	Proteolysis	SpI	5/5
Q8CW43	OmpW	Outer membrane protein W	Unknown	SpI	3/5
Q1REB0	OmpX	Outer membrane protein X	Unknown	SpI	4/5
Q8CW11	SlyB	Outer membrane lipoprotein	Unknown	SpII	4/5
Q1RDE2	Flu	Antigen 43 autotransporter	Autoaggregation	SpI	5/5
Unknown					
Q1RGG7	CarB	Carbamoyl-phosphate synthase large chain	Nucleotide metabolism	CYT	5/5
B3HX45	Mdh	Malate dehydrogenase	Organic compound metabolism	SpI	5/5
Q1RGJ5	TalB	Transaldolase B	Organic compound metabolism	CYT	4/5
Q0TFS5	PsuG	Putative uncharacterised protein	Cellular processes	CYT	1/4
Q8FBD4	SodA	Superoxide dismutase	Cellular processes	CYT	2/5
D6JHU3	RplL	50S ribosomal protein L7/L12	Translation	CYT	1/5
D6J8X1	WrbA	NAD(P)H:quinone oxidoreductase	Regulation, cellular processes	CYT	1/5
Q8GA08	Hek	Adhesin/virulence factor	Unknown	SpI	3/3
B1IQT1	MlaC	ABC transporter maintaining OM asymmetry	Unknown	SpI	3/5
Q1R227	UTI89_P011	Putative exported protein	Unknown	SpI	2/3
Q1RFK8	UTI89_C0355	Putative ribose ABC transporter	Unknown	SpI	2/2
Q8FHZ4	YchN	Putative uncharacterised protein	Unknown	CYT	3/5
Q1RBM1	YdfZ	Putative uncharacterised protein	Unknown	CYT	2/2
Q8CW30	YncE	Putative uncharacterised protein	Unknown	SpI	4/5
Periplasmic					
Q8CVK7	DppA	Periplasmic dipeptide transport protein	Transport	SpI	4/5
D2NES2	MalE	Maltose ABC transporter protein	Carbohydrate transport	SpI	4/5
D6J882	Pgl	6-Phosphogluconolactonase	Carbohydrate metabolism	CYT	4/5
D6IPI4	Tpx	Thiol peroxidase	Cellular processes	CYT	4/5
D6J8Y7	ECP_1017	Putative imelysin-like protein	Unknown	SpI	4/5
Cytoplasmic					
Q1R5J3	Asd	Aspartate-semialdehyde dehydrogenase	Amino acid metabolism	CYT	5/5
Q304P7	AspC	Aspartate aminotransferase	Amino acid metabolism	CYT	5/5
D6J627	DapD	Tetrahydrodipicolinate N-succinyltransferase	Amino acid metabolism	CYT	5/5
D6I9Y8	GlyA	Serine hydroxymethyltransferase	Amino acid metabolism	CYT	5/5
D6JH90	IlvD	Dihydroxy-acid dehydratase	Amino acid metabolism	CYT	5/5
Q0TLR6	LeuB	3-Isopropylmalate dehydrogenase	Amino acid metabolism	CYT	5/5
Q1RB13	GapA	Glyceraldehyde-3-phosphate dehydrogenase A	Carbohydrate metabolism	CYT	5/5
Q1R4K6	GlmS	Glucosamine-6-phosphate synthase	Carbohydrate metabolism	CYT	5/5
Q1R3Z2	GlpK	Glycerol kinase	Carbohydrate metabolism	CYT	4/5
Q1R5N2	PckA	ATP phosphoenolpyruvate carboxykinase	Carbohydrate metabolism	CYT	5/5
C6UM75	AceE	Pyruvate dehydrogenase subunit	Cellular processes	CYT	4/5
D3GXX4	UxuB	D-Mannonate oxidoreductase	Cellular processes	CYT	4/5
Q8X6U4	YliJ	Putative transferase	Cellular processes	CYT	4/5
D6J5F5	PurA	Adenylosuccinate synthetase	DNA Metabolism	CYT	5/5
D6JEB0	Eno	Phosphopyruvate hydratase	Energy metabolism	CYT	4/5
B7MPL3	GltA	Citrate synthase	Energy metabolism	CYT	5/5

Table 2 (*continued*)

Accession	Protein	Description/annotation[a]	Functional classification[b]	LipoP[c]	Prevalence[d] (detected protein/gene)
Q1REH6	GpmA	Phosphoglycerate mutase 1	Energy metabolism	CYT	4/5
Q9KH99	Icd	Isocitrate dehydrogenase [NADP]	Energy metabolism	CYT	5/5
Q1RG75	LpdA	Dihydrolipoyl dehydrogenase	Energy metabolism	CYT	5/5
Q1R7A7	Pgk	Phosphoglycerate kinase	Energy metabolism	CYT	5/5
Q707L6	GlcB	Malate synthase	Organic compound metabolism	CYT	4/5
Q65A08	UxuA	Mannonate hydrolase	Organic compound metabolism	CYT	5/5
Q1REV6	AhpC	Alkyl hydroperoxide reductase, C22 subunit	Stress response	CYT	5/5
D6JGC4	FusA	Translation elongation factor G	Translation	CYT	5/5
D6JGA3	RplC	50S ribosomal protein L3	Translation	CYT	4/5
D6JG91	RplE	50S ribosomal protein L5	Translation	CYT	5/5
D6J631	Tsf	Translation elongation factor Ts	Translation	CYT	5/5
D5D637	Tuf	Elongation factor Tu	Translation	CYT	5/5

Proteins are organised according to their subcellular location as predicted by the PSORTb algorithm [35]. All identified extracellular, outer membrane and proteins of unknown subcellular location are included, as well as prevalent (detected in ≥80% of strains) periplasmic and cytoplasmic proteins.

[a] UniProt protein annotation [34].

[b] Functional classification according to ontology [78].

[c] LipoP prediction [36]; CYT: cytoplasmic, TMH: transmembrane helix, SPI: classic signal peptide, SPII: lipoprotein signal peptide.

[d] Prevalence of detected proteins and corresponding genes in the five reference UPEC strains.

3. Results

3.1. Mass spectrometric analysis of proteolytic peptides and proteins of UPEC produced during growth in human urine

The OMV proteome of five reference UPEC strains (536, CFT073, F11, UMN026 and UTI89) was determined following culture in human urine at 37 °C using a combination of EDTA heat-induced OMVs and nanoLC–MS/MS. Mass spectrometric analysis detected 3569 unique peptide sequences with a confidence interval (CI) ≥95%, originating from 501 proteins (mean: 7.1 ± 12.9 high confidence peptides per protein), for an average of 100.6 ± 30.0 proteins per strain (Table S2). This equated to a non-redundant set of 173 unique proteins (Tables 2 and S2). Proteomic and genetic profiles were congruent, *i.e.* identified proteins were detected in strains positive for the corresponding gene (Table S2).

3.2. Subcellular distribution of UPEC proteins identified following growth in human urine

The subcellular origin of identified proteins and corresponding peptides was analysed *in silico* using the PSORTb algorithm [35]. Of the 3569 high confidence peptide sequences detected, 644 (18%) originated from extracellular proteins, 1332 (37%) from OM proteins, 219 (6%) from proteins of unknown subcellular location, 205 (6%) from periplasmic proteins and 1169 (33%) from cytoplasmic proteins (Fig. 1A). No inner membrane specific peptide sequences (CI ≥ 95%) were detected. Since proteins were typically identified by more than one high confidence peptide hit, subcellular fraction ratios varied between identified peptide sequences and identified proteins (Fig. 1A). The 501 redundant proteins consisted of 24 (5%) extracellular, 91 (18%) OM, 38 (8%) proteins of unknown origin, 50 (10%) periplasmic and 298 (59%) cytoplasmic proteins, for an average of 4.8 ± 1.1 extracellular, 18.6 ± 2.1 OM, 7.6 ± 3.2 proteins of unknown origin, 10.0 ± 4.7 periplasmic and 59.6 ± 24.3 cytoplasmic proteins per strain. The non-redundant library of 173 unique proteins consisted of 8 (5%) extracellular, 23 (13%) OM, 14 (8%) unknown, 21 (12%) periplasmic and 107 (62%) cytoplasmic proteins (Table S2). LipoP analysis predicted either a classic signal peptide sequence (SP I) or a lipoprotein signal peptide sequence (SP II) in 43% of proteins of unknown origin, suggesting that they did not originate from the cytoplasm (Fig. 1, Table 2).

The number of identified proteins was compared to the total number of proteins in the predicted bacterial proteome for each strain (Fig. 1B). In a subcellular context, a relatively large fraction of predicted OM proteins was identified (16–19%), whereas up to 10% and 9% of the predicted extracellular and periplasmic proteome were detected, respectively (Fig. 1B). Comparatively few cytoplasmic and proteins of unknown origin were detected.

3.3. Virulence and surface proteins produced by UPEC during growth in human urine

The OMV proteomic analysis of the five UPEC strains grown in human urine identified 37 surface proteins, some of which are linked to UPEC virulence (Table 2, Fig. 2). Peptide sequences specific to the porin proteins OmpA, OmpC, OmpF, NmpC and UidC were ubiquitous in the OMV proteomes of the UPEC strains examined. Other identified surface proteins with conserved cognate genes in all five strains included the protease VII protein OmpT (detected in all strains), OmpX and the lipoprotein SlyB (detected in 4/5 strains), and OmpW (detected in 3/5 strains). The vitamin B-12 receptor BtuB and colicin I sensitive receptor CirA were detected in 5/5 and 4/5 strains, respectively.

Multiple surface proteins corresponding to virulence factors were detected, including iron acquisition receptors, toxins and adhesins. Peptide sequences specific to eleven distinct iron acquisition receptors were identified, including two putative iron receptor proteins. The haem/haemoglobin receptor ChuA was identified in all five strains, as were the ferrienterobactin receptor FepA and the yersiniabactin receptor FyuA. The catecholate siderophore receptor Fiu and the salmochelin receptor IroN were detected in 4/5 and 4/4 strains positive for the corresponding gene, respectively (Fig. 2). Peptide sequences specific to the putative siderophore receptor CjrC, the siderophore receptor Iha and the ferric aerobactin receptor IutA were detected in 2/2 strains containing the corresponding genes; the putative iron transport receptor UTI89_C2234 was detected in 3/4 strains. Peptides corresponding to the ferrichrome-iron receptor FhuA were detected in 2/5 *fhuA* positive strains; a single strain contained the DNA and peptide sequences specific to the siderophore receptor IreA. Co-expression of multiple iron receptor proteins was observed in all strains (mean: 7.6 ± 1.7 iron receptors per strain), with up to nine distinct iron uptake receptor proteins identified in the OMV proteome of CFT073 and UTI89 (Fig. 2).

Peptides corresponding to the flagellar filament subunit protein FliC were detected in 4/5 strains containing the corresponding gene, the haemolysin toxin HlyA was detected in 3/4 strains containing *hlyA* and the accessory colonisation factor SslE was observed in 2/4 isolates positive for *sslE* (Fig. 2). Several distinct adhesins were detected, including the antigen 43 (Ag43) autotransporter protein (detected in all strains), and the neonatal meningitis *E. coli* (NMEC) Hek adhesin protein, which was detected in strains 536, F11 and UTI89. The *hek* gene is absent from the genome of CFT073 and UMN026. Hypothetical exported protein UTI89_P011 was detected in 2/3 strains positive for the analogous gene.

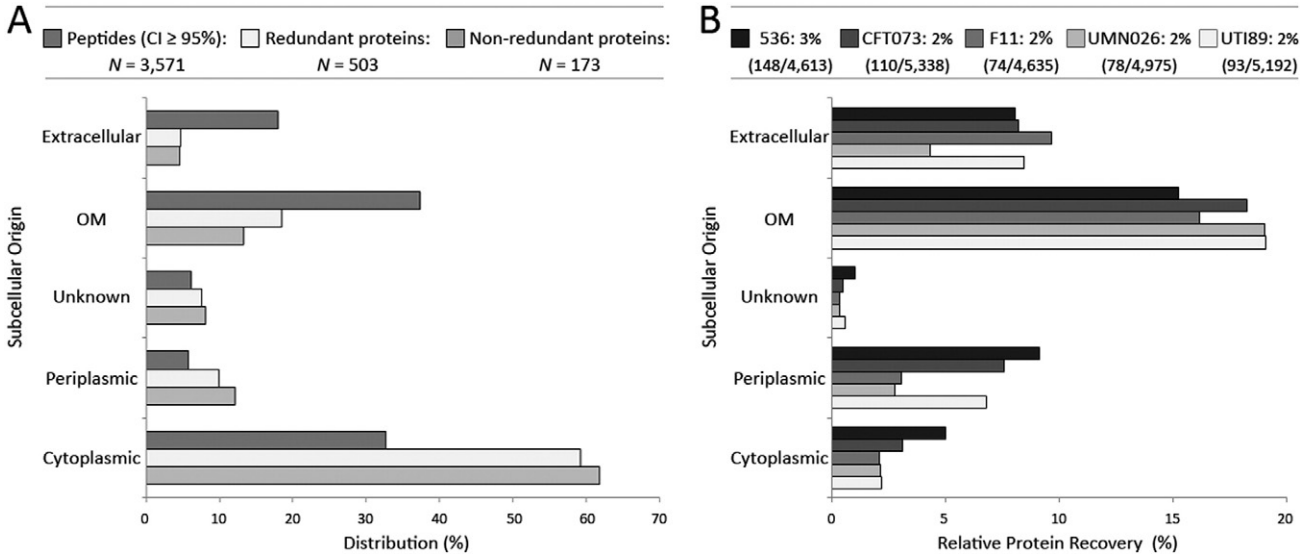

Fig. 1. Subcellular distribution and recovery rates of detected peptides and proteins. Peptides and proteins were identified by nanoLC–MS/MS of EDTA heat-induced OMVs isolated from five UPEC strains cultured in urine. Protein subcellular locations were predicted with PSORTb [35] and defined as Extracellular, Outer-membrane (OM), Unknown, Periplasmic or Cytoplasmic. (A) Location-based distribution of identified peptides, redundant proteins and non-redundant proteins, displayed as a percentage of the total number of peptides/proteins detected. A large fraction of identified peptide sequences originated from OM, cytoplasmic and extracellular proteins. (B) Per strain protein recovery rate relative to the complete proteome in a subcellular location-based arrangement. The total percentage of proteins recovered per strain is displayed at the top of the figure, with the number of identified/total number of proteins displayed in parentheses. Up to 19% of predicted OM and 10% of extracellular proteins were recovered, whereas relatively few cytoplasmic or proteins of unknown subcellular origin were detected. No high confidence peptides corresponding to inner membrane proteins were detected.

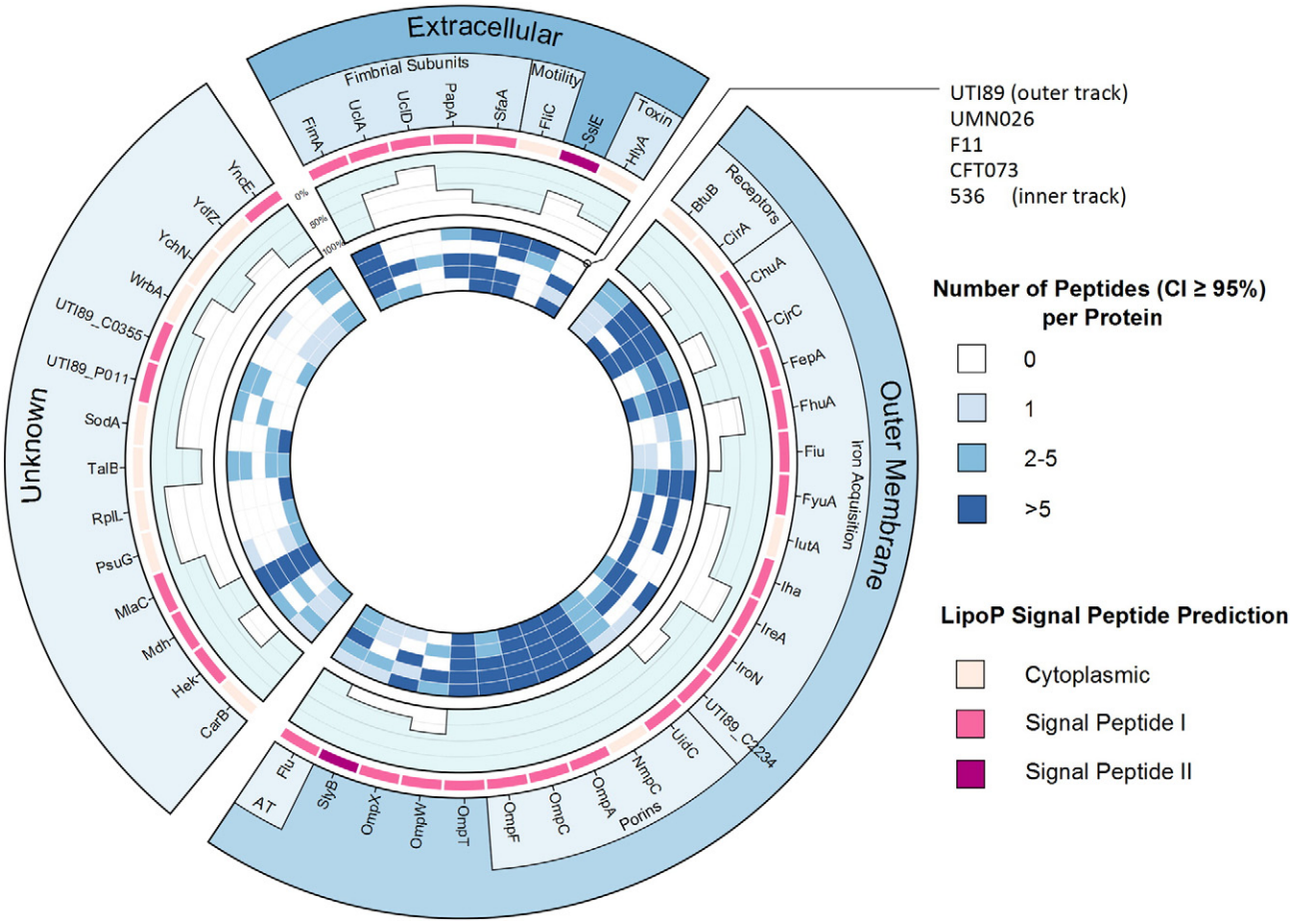

Fig. 2. Prevalence and distribution of surface proteins identified in five UPEC strains during growth in human urine. Outer ring groups: proteins of extracellular, OM and unknown subcellular origin as predicted by the PSORTb algorithm [35], and highlighted according to function where this is known (AT: autotransporter). Signal peptide sequences were predicted using LipoP [36] and displayed in pink to magenta as described in the key. The histogram in blue displays the prevalence in percentage of identified proteins in the five strains. The inner five rings represent a qualitative display of the number of high confidence peptides (CI ≥ 95%) detected per protein per strain as indicated in the key. The figure was created using the Circos software package [37].

Fimbrial subunit proteins from four distinct CU fimbrial types were identified in the proteomes of the UPEC strains examined (mean: 2.8 ± 1.1 fimbrial types per strain). Peptide sequences specific to the type 1 fimbriae major subunit FimA were detected in all strains, the F1C/S fimbriae major subunit SfaA was identified in 4/4 strains containing the F1C/S operon, and the P fimbriae major subunit PapA was detected in 3/5 strains positive for at least one *pap* operon. Peptides corresponding to the major subunit of a previously uncharacterised F17-like fimbrial type were detected in UPEC strains F11 and 536 (Fig. 2). Based on their phylogeny described in the remainder of this work, these fimbriae have been termed UCL (UCA-like) fimbriae. Peptide sequences identified by mass spectrometry covered 100% (160/160 aa, 22 high confidence peptides) and 22% (35/160 aa, 2 high confidence peptides) of the UclA predicted mature major subunit protein in *E. coli* F11 and 536, respectively (Fig. 3). Additionally, peptides corresponding to the UCL adhesin protein UclD were detected in F11 and covered 20% (67/339 aa, 4 high confidence peptides) of the predicted mature protein. While the *ucl* operon is also present in UTI89, no UCL specific peptide sequences were detected in the OMV proteome of this strain under the conditions examined in this study.

3.4. Evolutionary phylogeny and genomic organisation of UCL fimbriae

In a previous study on the identification and phylogenetic classification of CU fimbriae in the *E. coli* pan-genome, we classified UCL fimbriae (previously annotated as F17-like or UCA-like fimbriae) as a PAI-associated gamma 4 fimbrial type exclusively found in UPEC strains [22]. In order to investigate the distribution of the *ucl* operon among Gram-negative bacteria, genomes available on the NCBI database were probed using the BLASTp and tBLASTn algorithms for the UCL major subunit (Q1R2V4), chaperone (Q1R2V5), usher (Q1R2V6) and adhesin (Q1R2V7) amino acid and cognate nucleotide sequences. A phylogenetic tree based on UCL-related usher protein sequences was constructed to evaluate the UCL evolutionary history and combined with DNA alignments of the genomic context of the corresponding fimbrial operons to determine genetic conservation. The *ucl* gene cluster was detected in four complete *E. coli* genomes, namely UPEC strains 536 (ECP_3785–3782), F11 (EcF11_0745–0748) and UTI89 (UTI89_C4907–C4904) as well as asymptomatic bacteriuria (ABU) *E. coli* strain 83972 (ECABU_c48670–c48640). The *ucl* operon is 4957 nucleotides in length and consists of four structural genes arranged in polycistronic conformation, encoding, from 5′ to 3′: the major subunit (*uclA*), chaperone (*uclB*), usher (*uclC*) and adhesin (*uclD*) (Fig. 4). No partial/disrupted *ucl* related DNA sequences were discovered. Based on usher protein sequence phylogeny, UCL fimbriae form a monophyletic clade, which is closely related to UCA fimbriae from *P. mirabilis* (PMI0536–PMI0533) and an uncharacterised fimbrial type in *E. coli* KTE194 (A13Y_00037–00040), whereas they are relatively more distantly related to F17/G fimbriae (pVir_8–11) in *E. coli* (Fig. 4). In this scheme, the mean evolutionary distance between the UCA and UCL fimbrial usher protein is 0.22 ± 0.02 amino acid substitutions per site over 808 positions, which is similar to the evolutionary divergence of P and Pix fimbriae (0.28 ± 0.05 substitutions/site, 808 positions) [22,44]. The estimated evolutionary divergence between UCL and F17/G fimbriae comprises 1.41 ± 0.05 substitutions per site over an equal number of amino acid positions.

To evaluate the conservation of UCL fimbriae in *E. coli*, individual UCL structural subunit proteins from strains 536, F11, UTI89 and 83972 were investigated for sequence variation. The mean estimated evolutionary divergence between UCL usher proteins equals 0.006 ± 0.002 amino acid substitutions per site over 837 positions, while the chaperone divergence rate equates to 0.005 ± 0.003 substitutions per site (237 positions). The UCL adhesin protein exhibits a high degree of conservation, with 0.001 ± 0.001 amino acid substitutions per site over 359 positions, involving a single isoleucine to threonine mutation at position 259 in the C-terminal domain of $UclD_{83972}$. The estimated mean evolutionary divergence between the UCL and UCA adhesin protein equals 0.235 ± 0.026 amino acid substitutions over 359 positions, which is similar to the evolutionary distance based on usher protein phylogeny. The UclA major subunit is the least conserved UCL structural protein, with an evolutionary divergence of 0.187 ± 0.025 amino acid substitutions per site over 182 positions. As UclA sequences of *E. coli* F11, UTI89 and 83972 are identical, the relatively high degree of diversity of the UCL major subunit is exclusively due to sequence variation of $UclA_{536}$. Based on protein phylogeny, the closest homologue to $UclA_{536}$ is the major subunit of the UCA-like uncharacterised fimbrial type in *E. coli* KTE194 (A13Y_00037). Apart from UclA, UCL fimbrial gene products form monophyletic groups and display a low degree of variation, demonstrating that UCL fimbriae are generally well conserved.

The chromosomal location of the *ucl* operon comprises a highly conserved 5′ region, which contains four ORFs including a putative *tetR*-like regulator (Fig. 4). The 3′ region is somewhat more variable and contains a putative *luxR*-like regulator in *E. coli* F11, UTI89, and 83972 or a putative *papX*-like regulator in 536. Like the *uca* regulator immediately

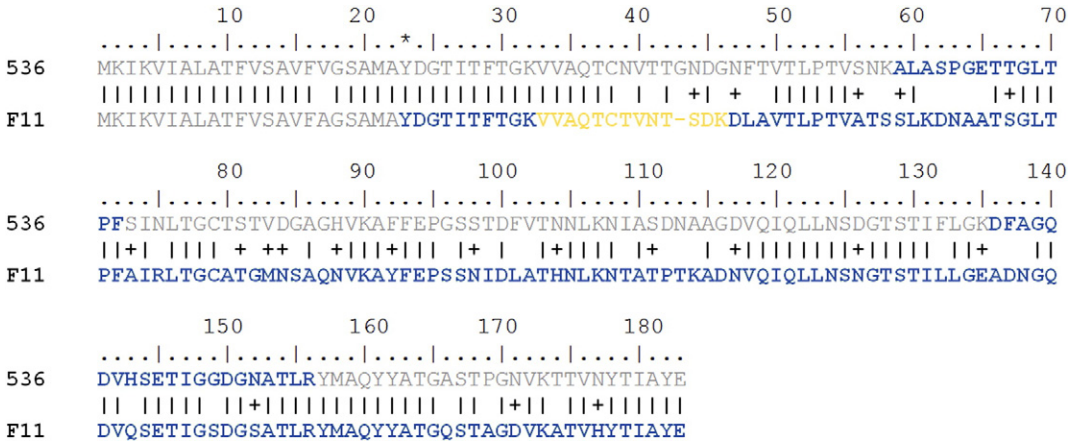

Fig. 3. Alignment and mass spectrometric sequence coverage of UclA from UPEC strains 536 and F11. Amino acid sequence alignment of the unprocessed UCL major subunits $UclA_{536}$ and $UclA_{F11}$; '+' symbols represent conserved amino acid substitutions. The asterisk at position 23 marks the first amino acid after the signal peptide cleavage site as predicted by LipoP [36]. Amino acid residues highlighted in blue represent peptide hits (CI ≥ 95%) detected by nanoLC–MS/MS in the OMV proteome of the corresponding strain. Sequences in yellow represent a peptide hit with a lower confidence score (69%), and residues in grey were not detected by tandem mass spectrometry. 22% and 100% of the predicted mature UclA protein sequence (160 residues) were detected in strains 536 and F11, respectively. The UclA major subunit is the least conserved UCL structural protein. Since UclA protein sequences of *E. coli* F11, UTI89 and 83972 are identical, the relative high degree of variation of the UCL major subunit is exclusively due to sequence diversity of $UclA_{536}$.

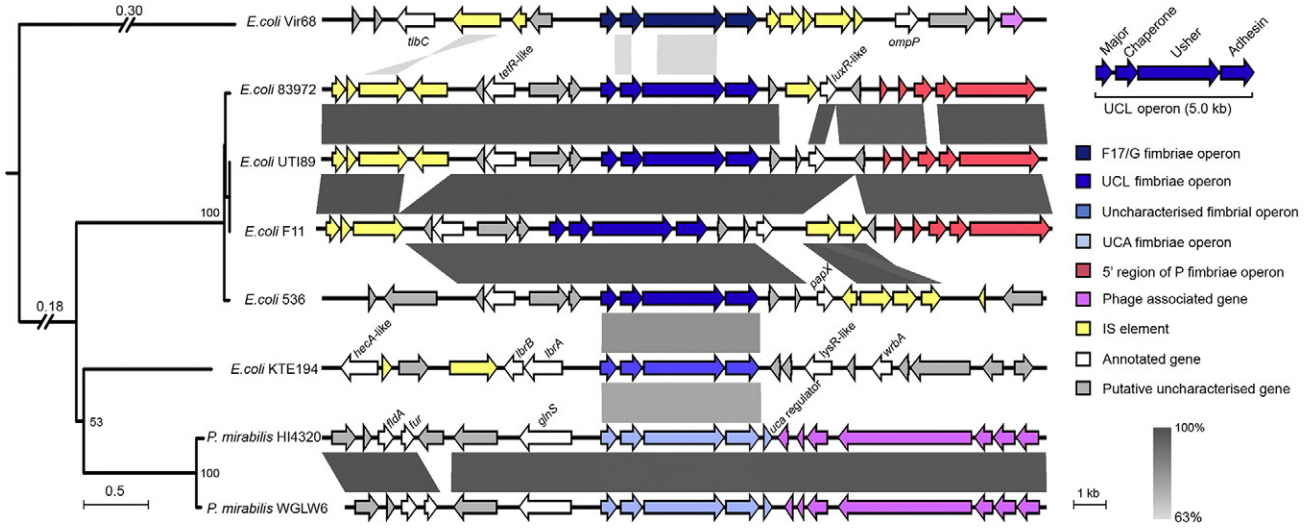

Fig. 4. Evolutionary phylogeny and genetic organisation of UCL fimbriae. Left: The evolutionary phylogeny of UCL and related fimbriae was inferred using the Neighbour-Joining method on usher amino acid sequences and evaluated using a 1000 replicate Bootstrap test displayed as percentage on major nodes. The scale represents the number of amino acid substitutions per site over 808 positions. The phylogenetic tree was visualised with iTOL [39]. Right: Alignment and genomic context of F17/G, UCL, KTE194 A13Y_00037–00040 and UCA fimbriae (highlighted in dark blue to light blue, respectively), with corresponding bacterial strains marked on the left of the alignment. The genomic context scale represents DNA length in kilobase pair, DNA sequence similarity is indicated in grey as percentage identity. UCL and related fimbrial operons are flanked by transposable elements (yellow) or phage encoding genes (purple) and are associated with plasmids (F17/G) or PAIs (UCL, KTE194 A13Y_00037–00040), suggesting this fimbrial clade is involved with horizontal gene transfer.

downstream of the *uca* operon in *P. mirabilis*, a conserved ORF is located directly downstream of *uclD*. However, this ORF shares no significant sequence similarity with the *uca* regulator or any other characterised genes.

As previously reported, UCL fimbriae are associated with PAIs; the *ucl* operon is located 3.8 kb upstream of the P fimbrial operon on the PAI-*leuX* in *E. coli* F11, UTI89 and 83972, whereas it resides on PAI-*selC* in *E. coli* 536 [22,45]. Typical for mobile genetic elements, the GC content of the *ucl* operon (mean: 42.1% ± 0.1) differs from the mean genomic GC content of the four corresponding *E. coli* strains (mean: 50.6% ± 0.1). UCL encoding genes are flanked by insertion sequence elements approximately 4.7 kb upstream of *uclA* and between 1.4 and 3.0 kb downstream of *uclD* (Fig. 4). UCL-related fimbrial operons are likewise associated with mobile genomic elements; *E. coli* KTE194 A13Y_00037–00040 resides on PAI-*pheU* and is flanked upstream by insertion sequences, prophage φ-PMI0456–PMI0530 is located directly downstream of the *uca* operon of *P. mirabilis* and the plasmid-borne F17/G fimbrial gene cluster is flanked by insertion sequences and prophage related genes (Fig. 4).

3.5. Prevalence of ucl genes in E. coli

Seventy-two strains of the diverse and well-characterised *E. coli* reference (ECOR) collection, as well as a diverse in-house collection of fifty-one urosepsis UPEC isolates were screened by PCR for the presence of UCL encoding genes. Based on the genomic analysis described above, primers were designed in conserved regions of the *ucl* operon to screen for the major subunit/chaperone (*uclA*, *uclB*), usher (*uclC*) and adhesin (*uclD*) genes (primers listed in Table S2). Consistent with the finding of the genomic analysis, genomic integrity of the *ucl* operon was conserved and strains either possessed or lacked all of the *ucl* genes screened by PCR, with no partial subunit conformations observed. In the ECOR collection, 10% (7/72) of strains screened positive for the *uclABCD* genes (strains ECOR48, ECOR51, ECOR52, ECOR53, ECOR54, ECOR60, ECOR63). The *uclABCD* genes were significantly more prevalent in the urosepsis UPEC collection (present in 15/51 [29%] strains, $P < 0.01$).

While the *E. coli* species is highly genetically diverse, strains can be grouped into 5 major monophyletic clades (phylogroups A, B1, B2, D and E) [46]. UPEC strains are typically members of phylogroups B2 and D. PCR data from both ECOR and urosepsis UPEC collections were merged to evaluate *ucl* operon prevalence in a phylogenetic context. The *ucl* operon was present in 40% (19/48) and 11% (3/27) of B2 and D isolates, respectively, but absent in phylogroup A ($n = 26$), B1 ($n = 18$) and E ($n = 4$) strains. Together, these data demonstrate that UCL fimbriae are primarily found in UPEC strains and are strongly associated with *E. coli* phylogenetic groups B2 and D.

3.6. Morphology of UCL fimbriae

CU fimbriae are frequently associated with *E. coli* adherence and biofilm formation. To investigate whether UCL fimbriae mediate these phenotypes, the complete *uclABCD* gene cluster from UPEC strain 536 was PCR amplified and cloned under the control of the *lac* promoter (plasmid pUCL). *E. coli* strain MS428 [47] transformed with pUCL or pSU2718 (vector control) was cultured in the presence of 1 mM IPTG and examined by electron microscopy to confirm fimbrial production on the cell surface. Negatively stained *E. coli* MS428(pUCL) cells contained relatively long, thin, flexible fimbrial structures uniformly distributed on their surface (Fig. 5A–C), while no fimbrial structures were observed on MS428 cells containing pSU2718 (Fig. 5D).

3.7. UCL fimbriae mediate biofilm formation on abiotic surfaces

The ability of UCL fimbriae to mediate biofilm formation was evaluated using a high throughput microtitre plate assay and a continuous flow chamber system. The UCL-overexpressing recombinant *E. coli* strain MS428(pUCL) formed a strong biofilm ($OD_{595} = 3.15 \pm 0.11$) on PVC microtitre plates when cultured at 37 °C in M9 medium (Fig. 6A). No substantial biofilm ($OD_{595} = 0.4 \pm 0.06$) was produced by vector control strain MS428(pSU2718). Using a continuous-flow chamber system in combination with a *gfp*-tagged derivative of *E. coli* MS428 (*i.e. E. coli* OS56), the ability of UCL fimbriae to promote biofilm formation under dynamic conditions was examined. UCL-expressing *E. coli* OS56(pUCL) produced a dense and uniform biofilm significantly increased in biovolume, substratum coverage and mean thickness compared to the vector control strain OS56(pSU2718) ($P < 0.001$; Fig. 6B).

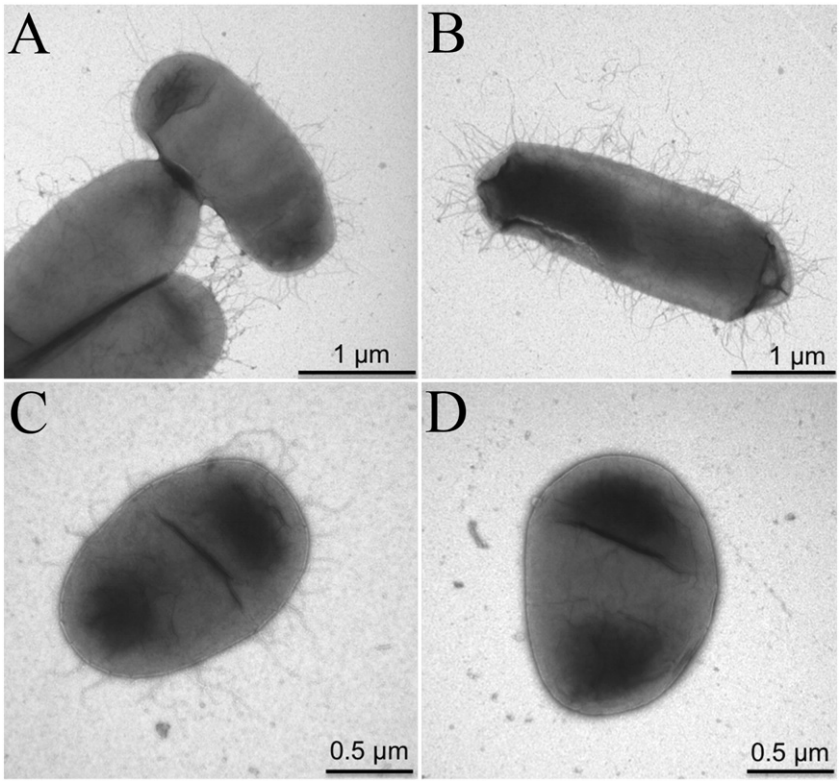

Fig. 5. UCL fimbriae are organised as flexible thin hair-like structures on the cell surface of *E. coli*. Transmission electron micrographs of (A–C) UCL-expressing *E. coli* strain MS428(pUCL) and (D) control *E. coli* strain MS428(pSU2718) negatively stained with 1% uranyl acetate. Cells were obtained from overnight cultures at 37 °C in LB media supplemented with 1 mM IPTG.

Combined, these data demonstrate that UCL fimbriae promote strong biofilm formation in two distinct biofilm model systems.

3.8. UCL fimbriae mediate adherence to exfoliated human uroepithelial cells

The UCL fimbrial operon is unique to UPEC and its constituent subunit proteins were detected following growth of UPEC F11 (UclA and UclD) and 536 (UclA) in human urine. To investigate whether UCL fimbriae recognise epitopes on cells of the urinary tract, exfoliated human uroepithelial cells were mixed with UCL overexpressing *E. coli* and examined for adherence. Desquamated epithelial cells were collected from the mid-stream urine of four healthy female volunteers, incubated with MS428(pUCL, pCO13) (*gfp*-tagged strain expressing UCL fimbriae) or MS428(pSU2718, pCO13) (*gfp*-tagged negative control strain) and examined by epifluorescence/light microscopy. In this assay, UCL-expressing *E. coli* strain MS428(pUCL, pCO13) attached in

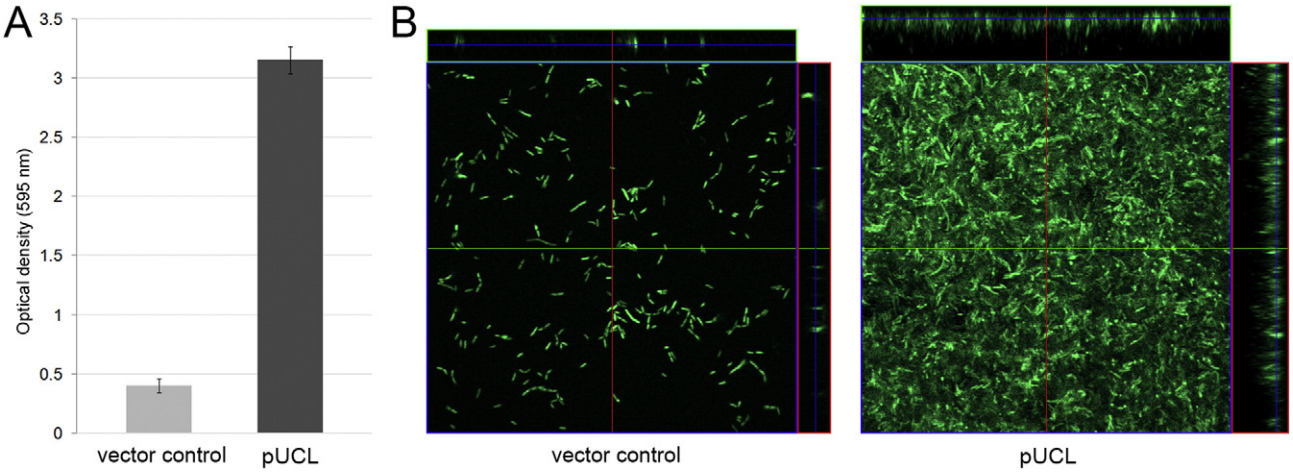

Fig. 6. UCL fimbriae mediate *E. coli* biofilm formation on abiotic surfaces. (A) PVC microtitre plate biofilm formation assay of MS428 containing vector control plasmid pSU2718 or UCL fimbriae expression plasmid pUCL after 24 h growth at 37 °C in M9 medium. The optical density at 595 nm is an indication of biofilm formation (displayed as mean ± SD). MS428(pUCL) formed a significantly stronger biofilm ($P < 0.001$) in comparison with vector control strain MS428(pSU2718). (B) Dynamic flow chamber assay displaying spatial distribution and biofilm formation on a glass surface of the GFP^+ strain OS56 containing pSU2718 (vector control plasmid) or pUCL (UCL fimbriae expression plasmid) cultured in M9 medium for 24 h at 28 °C. The large panes illustrate representative horizontal flow cell cross sections (positioned at the blue line in the side panels); the smaller panes at the top and right represent vertical cross sections at the positions indicated by the red and green lines. The UCL-overexpression strain OS56(pUCL) produced a biofilm with a significant ($P < 0.001$) increase in total biovolume, substratum coverage and mean thickness compared to vector control strain OS56(pSU2718).

large numbers (>100 GFP^+ bacteria per eukaryotic cell) to exfoliated uroepithelial cells, while no adherence (<5 GFP^+ bacteria per eukaryotic cell) was observed by vector control strain MS428(pSU2718, pCO13) (Fig. 7). *E. coli* strains expressing UCL fimbriae adhered to 68–80% of uroepithelial cells (data from 3 independent experiments, 50 eukaryotic cells examined per experiment). We also examined the ability of UCL fimbriae to mediate binding of *E. coli* to T24 human bladder and A498 human renal epithelial cells, however no binding was observed (data not shown). Taken together, our data demonstrate that UCL fimbriae bind to human desquamated uroepithelial cells *via* interaction with structures either not present or not readily exposed on the surface of immortalised human bladder and kidney epithelial cells.

4. Discussion

Bacterial surface proteins are often associated with virulence, and in some cases can be targeted for the development of diagnostics and therapeutics. However, the extensive genotypic and phenotypic heterogeneity of the UPEC pathogroup makes identification of common surface proteins challenging. We previously described a high-throughput method for the rapid characterisation of the *E. coli* surface proteome based on nanoLC–MS/MS of EDTA heat-induced OMVs [31]. Here, we have employed this methodology to characterise the UPEC surface proteome during growth in human urine.

OMVs are 20–200 nm spherical structures secreted constitutively from the OM of Gram-negative bacteria and are inherently enriched in surface proteins compared to whole-cell proteomes [48,49]. Chemical heat treatment was used to induce OMV production from UPEC strains and associated proteins were identified by nanoLC–MS/MS. Based on PSORTb predictions [35], the majority (55%) of high confidence peptide sequences detected originated either from OM or extracellular proteins. Overall, the subcellular composition of the EDTA-heat induced OMV proteome isolated from UPEC grown in urine resembled that of UPEC cultured in minimal medium and the native OMV proteome of *E. coli* DH5α [31,49]. More specifically, the number of surface proteins identified in CFT073 corresponded to previous studies investigating CFT073 under similar conditions using traditional proteomic methods [50,51]. While these methods generally identified more OM proteins, extracellular proteins associated with the cell surface, including fimbrial subunits, were typically absent.

UPEC are genetically heterogeneous pathogens and express a diverse array of surface proteins and virulence factors dependent on gene repertoires and/or environmental conditions. Accordingly, a comparative proteomic approach was utilised to investigate multiple UPEC strains for the expression of common surface proteins and variability of virulence factors. A total of 14 surface proteins (FimA, BtuB, ChuA, FepA, FyuA, UidC, NmpC, OmpA, OmpC, OmpF, OmpT, Flu, CarB and Mdh) were detected in all strains, and represent the core surface proteome of the five UPEC strains examined in this study during growth in urine. The ubiquity and association with the bacterial cell surface of these proteins may provide a framework for novel and broadly protective therapeutic interventions against UPEC-mediated UTI. The expression of this core set of

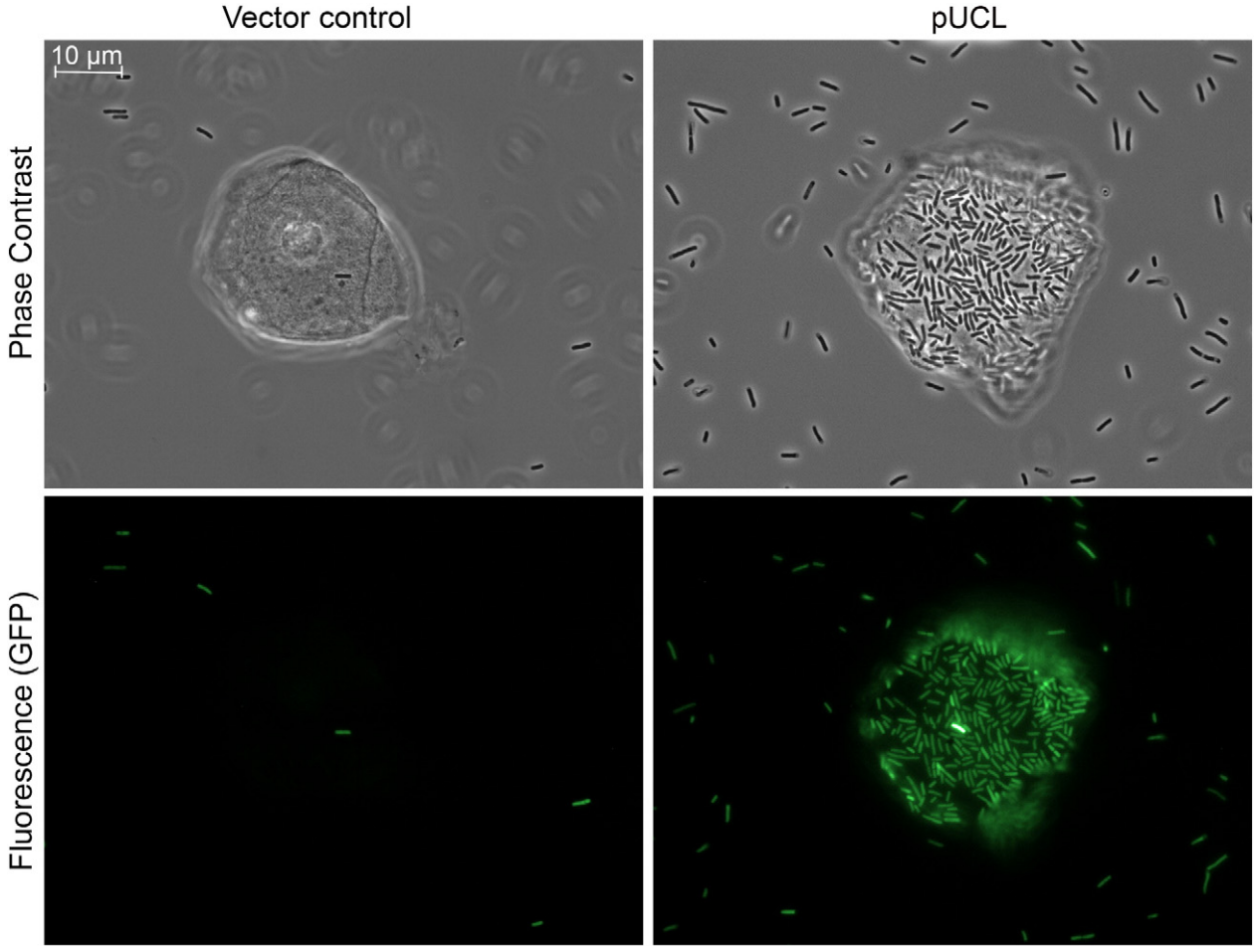

Fig. 7. UCL fimbriae mediate *E. coli* adherence to exfoliated human uroepithelial cells. Desquamated uroepithelial cells recovered from urine donated by four healthy female volunteers and infected with GFP^+ *E. coli* cells at a MOI of 10,000, incubated for 30 min at 37 °C, 100 rpm, thoroughly washed and examined by phase contrast (top) and fluorescent (bottom) microscopy. No substantial adherence was observed by vector control strain MS428(pSU2718, pCO13) (left). In contrast, UCL fimbriae-overexpressing strain MS428(pUCL, pCO13) adhered to 68%–80% of uroepithelial cells isolated from human urine, typically covering the complete uroepithelial cell surface (right). Data were collected from 3 independent experiments, 50 eukaryotic cells were examined per experiment.

surface proteins exhibited some differences when compared to a previous study performed following growth in M9 minimal medium [31] (*i.e.* ChuA, FepA, FyuA, NmpC, OmpA, OmpC, OmpF and OmpT were highly prevalent during both culture conditions, whereas FimA, BtuB, UidC, Flu, CarB and Mdh constitute core proteins after growth in urine only), suggesting specific regulatory control for at least some of the genes encoding these proteins.

Consistent with genome heterogeneity, the prevalence of identified virulence-associated proteins was variable, however, proteins associated with both iron uptake and adhesion were detected in all strains. As the urinary tract is iron-limited, iron-chelating siderophores and their cognate uptake systems enable UPEC to sequester this essential growth factor from the host. Secreted toxins including haemolysin and cytotoxic necrotising factor 1 cause extensive damage to tissues and immune effector cells, promoting bacterial dissemination, cell invasion, release of nutrients and suppression of host defence mechanisms [52–55]. Alpha-haemolysin is secreted either directly into the extracellular milieu or associated with OMVs and disseminated accordingly [56]. The haemolysin toxin HlyA was detected in three out of four UPEC isolates positive for the *hlyA* gene. Since *E. coli* 536 possesses two copies of the *hlyA* gene, the probability of detecting the corresponding protein using proteomic approaches may be increased in comparison with strains containing a single gene copy. Similar inferences may be made in respect to the detection of P fimbrial subunits in CFT073, which possesses two copies of the *pap* operon. The major flagellar filament subunit protein FliC was detected in four out of five strains containing the *fliC* gene, consistent with the notion that growth in urine may prime UPEC for flagella-mediated ascension to the upper urinary tract [57]. Eleven distinct iron uptake receptors were identified including the putative receptor proteins CjrC and UTI89_C2234. The *cjrC* gene is located on IncF conjugative plasmids in UTI89, UMN026 and F11 [28–30,58]. The *cjrABC* gene cluster has been associated with UPEC fitness during the early stages of acute cystitis in mice, however, the precise role of CjrC in uropathogenesis remains to be elucidated [58]. The UTI89_C2234 protein was detected in three out of four strains positive for the corresponding gene (*E. coli* CFT073, F11 and UTI89) and contains TonB-dependent haem/haemoglobin receptor and inorganic Fe transport domains. The co-expression of an average of 7.6 ± 1.7 iron receptors per strain exemplifies UPEC dependence on iron for growth in urine. Identified in all strains, the predicted porin protein UidC is part of the *uidABC* operon and involved in the active uptake of beta-glucuronosides, suggesting that UPEC actively acquires and metabolises glucuronosides secreted as a metabolic waste product by the kidneys [59]. UidA beta-glucuronidase is an intracellular hydrolase unique to *E. coli* that catalyses beta-glucuronosides, allowing the resulting glycone to be used as carbon source [59]. The secreted and surface-associated lipoprotein SslE is a strongly immunogenic and protective vaccine antigen in mice, and contributes to biofilm formation and gut colonisation by pathogenic *E. coli* [60–62]. SslE was detected in three strains after growth in human urine, suggesting that UPEC produces this protein during colonisation of the urinary tract and may be susceptible to SslE based vaccines. The Hek adhesin was detected in UPEC 536, F11 and UTI89 (CFT073 and UMN026 lack the *hek* gene). The *hek* gene is located on PAI-*leuX* directly downstream of the P fimbriae operon and is present in approximately 55% of UPEC strains [63]. This virulence factor mediates autoaggregation, adherence and invasion of T84 colonic cells by neonatal meningitis *E. coli* (NMEC) [64]. To the best of our knowledge, this is the first evidence of Hek expression by UPEC. Other adhesins identified included Ag43, which was detected in all strains and mediates autoaggregation, biofilm formation on abiotic surfaces, IBC formation and enhanced colonisation of the murine bladder epithelium [12,47,65].

UPEC utilise CU fimbriae as primary adherence factors for the colonisation of the human urinary tract. While type 1, P, F1C/S and AFA fimbriae are common fimbrial adhesins associated with UTI, the large diversity of adhesin-encoding genes in UPEC suggests that other fimbriae may also contribute to this phenotype. Based on peptide sequences corresponding to major subunit proteins, four distinct fimbriae types were identified during growth in urine, including the previously uncharacterised UCL fimbriae, which were detected in two out of three strains positive for the *ucl* operon (F11 and 536). Besides this new fimbrial type, major subunit proteins of type 1 fimbriae were detected in all strains, F1C/S fimbriae were detected in four strains and P fimbriae were detected in three out of five strains. The F1C/S operon in the F11 genome is annotated as disrupted due to a single point mutation in the usher-encoding gene, however the detection of the F1C major subunit in the F11 OMV proteome suggests that this operon is expressed in this strain and potentially functional. Co-production of multiple distinct fimbriae was observed in all UPEC strains. UPEC have been shown to coordinate fimbrial expression to limit the production of multiple fimbrial types on the cell surface [66,67]. Phase variation of several fimbrial operons in UPEC results in isogenic bacterial subpopulations expressing functionally distinct fimbriae, presumably to increase the probability of adherence to host tissues in the diverse niches of the human urinary tract [68]. As our proteomic analysis is at the population rather than the single cell level, it remains to be determined whether the identified fimbrial types are co-produced on the cell surface of these UPEC strains or produced by tightly regulated subpopulations.

We previously described that *E. coli* possess at least 38 distinct fimbrial types, some of which are associated with specific *E. coli* pathotypes [22]. UCL fimbriae (previously described as F17-like or UCA-like fimbriae [9,45,69]) were found exclusively in UPEC and are located within PAIs. In this study, we analysed the UCL genomic context, prevalence and phylogeny in order to investigate the conservation and evolutionary history of the *ucl* operon. The relatively low GC content, flanking insertion elements and PAI association suggest that UCL fimbriae were acquired *via* horizontal gene transfer [11]. Notably, the closely related UCA fimbriae of *P. mirabilis* and *E. coli* KTE194 (A13Y_00037–00040), as well as the more distantly related *E. coli* F17/G fimbriae, are also associated with mobile genetic elements. Based on the protein sequence phylogeny of UCL subunits, UCL fimbriae form a monophyletic clade, indicating that the ancestral UCL operon was acquired by an ancient *E. coli* lineage and subsequently disseminated among its extant *E. coli* descendants. The genetic mobility of the *ucl* genes is further emphasised by their location within PAI-*selC* (*E. coli* 536) or PAI-*leuX* (*E. coli* F11, UTI89, 83972). Additionally, the major subunit protein $UclA_{536}$ varies extensively in comparison with other UclA sequences, suggesting allelic replacement *via* recombination or considerable divergence of this protein during the evolutionary history of *E. coli* 536. The UclD adhesin protein is highly conserved, containing a single non-synonymous mutation in the C-terminal domain of the protein. The conservation of the lectin-recognising N-terminal domain implies that the binding properties of UCL fimbriae may be highly conserved. The direct 5′ and 3′ regions of the *ucl* operon contain multiple distinct ORFs homologous to characterised regulators, however there is currently no evidence linking these elements to the regulation of *uclABCD* transcription. Despite the presence of an apparently intact *ucl* fimbrial operon in UTI89, we did not detect expression of UCL fimbriae, suggesting differential regulation in this strain. This observation is consistent with a recent analysis of fimbrial expression in UTI89 following growth in LB broth [70,71]. There is currently no evidence for UCL fimbriae expression in ABU *E. coli* strain 83972.

The *ucl* fimbrial genes were identified in 29% of urosepsis *E. coli* isolates and exclusively found in members of phylogenetic groups B2 and D, which is consistent with the frequency of PAIs carrying the *ucl* operon in UPEC [72]. In addition to their association with UPEC strains, UCL fimbriae are closely related to UCA fimbriae from *P. mirabilis*, which mediate adherence to desquamated uroepithelial cells and play a role in the colonisation of the murine urinary tract by *P. mirabilis* [73,74]. Accordingly, UCL fimbriae were functionally characterised to determine a potential role in UPEC mediated uropathogenesis. We demonstrated that UCL fimbriae promote strong biofilm formation in two distinct

in vitro assays and mediate specific bacterial attachment to exfoliated uroepithelial cells when expressed in a recombinant *E. coli* strain. We did not detect any significant UCL-mediated binding of *E. coli* to T24 human bladder carcinoma or A498 human kidney carcinoma cells, and the target epitopes and precise role of UCL fimbriae in UPEC mediated UTI remain to be elucidated.

This study describes a comprehensive comparative characterisation of the UPEC surface proteome during growth in human urine. Our approach led to the identification of 14 core surface proteins, as well as the identification and characterisation of UCL fimbriae as a new PAI-associated fimbrial adhesin that mediates significant biofilm formation and confers specific adherence to human uroepithelial cells. Taken together, this study provides new insight into the composition of the UPEC surface proteome and highlights the potential contribution of UCL fimbriae in UPEC colonisation of the human urinary tract.

Supplementary data to this article can be found online at http://dx.doi.org/10.1016/j.jprot.2015.11.001.

Transparency Document

The Transparency document associated with this article can be found, in the online version.

Acknowledgements

This work was supported by grants from the National Health and Medical Research Council (NHMRC) of Australia (APP1042651, APP1068593, APP1067455 and APP1069370). MAS is supported by an NHMRC Senior Research Fellowship (APP1106930), MT by an ARC Discovery Early Career Researcher Award (DE130101169), and LPA by a Marie Curie Fellowship (PIIF-GA-2012-328261). We thank Dr. Alun Jones for the valuable technical assistance and expertise with the nanoLC–MS/MS.

References

[1] L. Zhang, B. Foxman, Molecular epidemiology of *Escherichia coli* mediated urinary tract infections, Front. Biosci. 8 (2003) e235–e244.
[2] B. Foxman, Epidemiology of urinary tract infections: incidence, morbidity, and economic costs, Am. J. Med. 113 (Suppl 1A) (2002) 5S–13S.
[3] W.E. Stamm, S.R. Norrby, Urinary tract infections: disease panorama and challenges, J. Infect. Dis. 183 (Suppl 1) (2001) S1–S4.
[4] B. Foxman, Recurring urinary tract infection: incidence and risk factors, Am. J. Public Health 80 (1990) 331–333.
[5] D.A. Tadesse, S. Zhao, E. Tong, S. Ayers, A. Singh, M.J. Bartholomew, et al., Antimicrobial drug resistance in *Escherichia coli* from humans and food animals, United States, 1950–2002, Emerg. Infect. Dis. 18 (2012) 741–749.
[6] B. Foxman, The epidemiology of urinary tract infection, Nat. Rev. Urol. 7 (2010) 653–660.
[7] N.K. Petty, N.L. Ben Zakour, M. Stanton-Cook, E. Skippington, M. Totsika, B.M. Forde, et al., Global dissemination of a multidrug resistant *Escherichia coli* clone, Proc. Natl. Acad. Sci. U. S. A. 111 (2014) 5694–5699.
[8] T.A. Russo, J.R. Johnson, Medical and economic impact of extraintestinal infections due to *Escherichia coli*: focus on an increasingly important endemic problem, Microbes Infect. 5 (2003) 449–456.
[9] E. Brzuszkiewicz, H. Bruggemann, H. Liesegang, M. Emmerth, T. Olschlager, G. Nagy, et al., How to become a uropathogen: comparative genomic analysis of extraintestinal pathogenic *Escherichia coli* strains, Proc. Natl. Acad. Sci. U. S. A. 103 (2006) 12879–12884.
[10] R.A. Welch, V. Burland, G. Plunkett 3rd, P. Redford, P. Roesch, D. Rasko, et al., Extensive mosaic structure revealed by the complete genome sequence of uropathogenic *Escherichia coli*, Proc. Natl. Acad. Sci. U. S. A. 99 (2002) 17020–17024.
[11] A.L. Lloyd, T.A. Henderson, P.D. Vigil, H.L. Mobley, Genomic islands of uropathogenic *Escherichia coli* contribute to virulence, J. Bacteriol. 191 (2009) 3469–3481.
[12] G.G. Anderson, J.J. Palermo, J.D. Schilling, R. Roth, J. Heuser, S.J. Hultgren, Intracellular bacterial biofilm-like pods in urinary tract infections, Science 301 (2003) 105–107.
[13] J.J. Martinez, M.A. Mulvey, J.D. Schilling, J.S. Pinkner, S.J. Hultgren, Type 1 pilus-mediated bacterial invasion of bladder epithelial cells, EMBO J. 19 (2000) 2803–2812.
[14] M.J. Kuehn, J. Heuser, S. Normark, S.J. Hultgren, P pili in uropathogenic *E. coli* are composite fibres with distinct fibrillar adhesive tips, Nature 356 (1992) 252–255.
[15] R. Selvarangan, P. Goluszko, J. Singhal, C. Carnoy, S. Moseley, B. Hudson, et al., Interaction of Dr adhesin with collagen type IV is a critical step in *Escherichia coli* renal persistence, Infect. Immun. 72 (2004) 4827–4835.
[16] I. Connell, W. Agace, P. Klemm, M. Schembri, S. Marild, C. Svanborg, Type 1 fimbrial expression enhances *Escherichia coli* virulence for the urinary tract, Proc. Natl. Acad. Sci. U. S. A. 93 (1996) 9827–9832.
[17] M. Totsika, D.G. Moriel, A. Idris, B.A. Rogers, D.J. Wurpel, M.D. Phan, et al., Uropathogenic *Escherichia coli* mediated urinary tract infection, Curr. Drug Targets 13 (2012) 1386–1399.
[18] D. Choudhury, A. Thompson, V. Stojanoff, S. Langermann, J. Pinkner, S.J. Hultgren, et al., X-ray structure of the FimC–FimH chaperone-adhesin complex from uropathogenic *Escherichia coli*, Science 285 (1999) 1061–1066.
[19] G. Phan, H. Remaut, T. Wang, W.J. Allen, K.F. Pirker, A. Lebedev, et al., Crystal structure of the FimD usher bound to its cognate FimC–FimH substrate, Nature 474 (2011) 49–53.
[20] E. Hahn, P. Wild, U. Hermanns, P. Sebbel, R. Glockshuber, M. Haner, et al., Exploring the 3D molecular architecture of *Escherichia coli* type 1 pili, J. Mol. Biol. 323 (2002) 845–857.
[21] P. Klemm, M.A. Schembri, Bacterial adhesins: function and structure, Int. J. Med. Microbiol. 290 (2000) 27–35.
[22] D.J. Wurpel, S.A. Beatson, M. Totsika, N.K. Petty, M.A. Schembri, Chaperone–usher fimbriae of *Escherichia coli*, PLoS ONE 8 (2013), e52835.
[23] C.H. Jones, J.S. Pinkner, R. Roth, J. Heuser, A.V. Nicholes, S.N. Abraham, et al., FimH adhesin of type 1 pili is assembled into a fibrillar tip structure in the *Enterobacteriaceae*, Proc. Natl. Acad. Sci. U. S. A. 92 (1995) 2081–2085.
[24] A.S. Khan, B. Kniep, T.A. Oelschlaeger, I. Van Die, T. Korhonen, J. Hacker, Receptor structure for F1C fimbriae of uropathogenic *Escherichia coli*, Infect. Immun. 68 (2000) 3541–3547.
[25] R. Marre, B. Kreft, J. Hacker, Genetically engineered S and F1C fimbriae differ in their contribution to adherence of *Escherichia coli* to cultured renal tubular cells, Infect. Immun. 58 (1990) 3434–3437.
[26] J. Miyazaki, W. Ba-Thein, T. Kumao, M. Obata Yasuoka, H. Akaza, H. Hayshi, Type 1, P and S fimbriae, and afimbrial adhesin I are not essential for uropathogenic *Escherichia coli* to adhere to and invade bladder epithelial cells, FEMS Immunol. Med. Microbiol. 33 (2002) 23–26.
[27] R.A. Welch, V. Burland, G. Plunkett 3rd, P. Redford, P. Roesch, D. Rasko, et al., Extensive mosaic structure revealed by the complete genome sequence of uropathogenic *Escherichia coli*, Proc. Natl. Acad. Sci. U. S. A. 99 (2002) 17020–17024.
[28] D.A. Rasko, M.J. Rosovitz, G.S. Myers, E.F. Mongodin, W.F. Fricke, P. Gajer, et al., The pangenome structure of *Escherichia coli*: comparative genomic analysis of *E. coli* commensal and pathogenic isolates, J. Bacteriol. 190 (2008) 6881–6893.
[29] M. Touchon, C. Hoede, O. Tenaillon, V. Barbe, S. Baeriswyl, P. Bidet, et al., Organised genome dynamics in the *Escherichia coli* species results in highly diverse adaptive paths, PLoS Genet. 5 (2009), e1000344.
[30] S.L. Chen, C.S. Hung, J. Xu, C.S. Reigstad, V. Magrini, A. Sabo, et al., Identification of genes subject to positive selection in uropathogenic strains of *Escherichia coli*: a comparative genomics approach, Proc. Natl. Acad. Sci. U. S. A. 103 (2006) 5977–5982.
[31] D.J. Wurpel, D.G. Moriel, M. Totsika, D.M. Easton, M.A. Schembri, Comparative analysis of the uropathogenic *Escherichia coli* surface proteome by tandem mass-spectrometry of artificially induced outer membrane vesicles, J. Proteome 115C (2014) 93–106.
[32] H. Ochman, R.K. Selander, Standard reference strains of *Escherichia coli* from natural populations, J. Bacteriol. 157 (1984) 690–693.
[33] G. Bertani, Studies on lysogenesis. I. The mode of phage liberation by lysogenic *Escherichia coli*, J. Bacteriol. 62 (1951) 293–300.
[34] E. Jain, A. Bairoch, S. Duvaud, I. Phan, N. Redaschi, B.E. Suzek, et al., Infrastructure for the life sciences: design and implementation of the UniProt website, BMC Bioinf. 10 (2009) 136.
[35] N.Y. Yu, J.R. Wagner, M.R. Laird, G. Melli, S. Rey, R. Lo, et al., PSORTb 3.0: improved protein subcellular localization prediction with refined localization subcategories and predictive capabilities for all prokaryotes, Bioinformatics 26 (2010) 1608–1615.
[36] A.S. Juncker, H. Willenbrock, G. Von Heijne, S. Brunak, H. Nielsen, A. Krogh, Prediction of lipoprotein signal peptides in Gram-negative bacteria, Protein Sci. 12 (2003) 1652–1662.
[37] M. Krzywinski, J. Schein, I. Birol, J. Connors, R. Gascoyne, D. Horsman, et al., Circos: an information aesthetic for comparative genomics, Genome Res. 19 (2009) 1639–1645.
[38] K. Tamura, D. Peterson, N. Peterson, G. Stecher, M. Nei, S. Kumar, MEGA5: molecular evolutionary genetics analysis using maximum likelihood, evolutionary distance, and maximum parsimony methods, Mol. Biol. Evol. 28 (2011) 2731–2739.
[39] I. Letunic, P. Bork, Interactive Tree Of Life (iTOL): an online tool for phylogenetic tree display and annotation, Bioinformatics 23 (2007) 127–128.
[40] M.J. Sullivan, N.K. Petty, S.A. Beatson, Easyfig: a genome comparison visualizer, Bioinformatics 27 (2011) 1009–1010.
[41] M.A. Schembri, P. Klemm, Biofilm formation in a hydrodynamic environment by novel fimh variants and ramifications for virulence, Infect. Immun. 69 (2001) 1322–1328.
[42] L.P. Allsopp, M. Totsika, J.J. Tree, G.C. Ulett, A.N. Mabbett, T.J. Wells, et al., UpaH is a newly identified autotransporter protein that contributes to biofilm formation and bladder colonization by uropathogenic *Escherichia coli* CFT073, Infect. Immun. 78 (2010) 1659–1669.
[43] A. Heydorn, A.T. Nielsen, M. Hentzer, C. Sternberg, M. Givskov, B.K. Ersboll, et al., Quantification of biofilm structures by the novel computer program COMSTAT, Microbiology 146 (Pt 10) (2000) 2395–2407.
[44] A. Lugering, I. Benz, S. Knochenhauer, M. Ruffing, M.A. Schmidt, The Pix pilus adhesin of the uropathogenic *Escherichia coli* strain X2194 (O2 : K(−): H6) is related to Pap pili but exhibits a truncated regulatory region, Microbiology 149 (2003) 1387–1397.

[45] U. Dobrindt, G. Blum-Oehler, G. Nagy, G. Schneider, A. Johann, G. Gottschalk, et al., Genetic structure and distribution of four pathogenicity islands (PAI I(536) to PAI IV(536)) of uropathogenic *Escherichia coli* strain 536, Infect. Immun. 70 (2002) 6365–6372.
[46] T. Wirth, D. Falush, R. Lan, F. Colles, P. Mensa, L.H. Wieler, et al., Sex and virulence in *Escherichia coli*: an evolutionary perspective, Mol. Microbiol. 60 (2006) 1136–1151.
[47] K. Kjaergaard, M.A. Schembri, C. Ramos, S. Molin, P. Klemm, Antigen 43 facilitates formation of multispecies biofilms, Environ. Microbiol. 2 (2000) 695–702.
[48] F. Berlanda Scorza, F. Doro, M.J. Rodriguez-Ortega, M. Stella, S. Liberatori, A.R. Taddei, et al., Proteomics characterization of outer membrane vesicles from the extraintestinal pathogenic *Escherichia coli* DeltatolR IHE3034 mutant, Mol. Cell. Proteomics 7 (2008) 473–485.
[49] E.Y. Lee, J.Y. Bang, G.W. Park, D.S. Choi, J.S. Kang, H.J. Kim, et al., Global proteomic profiling of native outer membrane vesicles derived from *Escherichia coli*, Proteomics 7 (2007) 3143–3153.
[50] M.S. Walters, H.L. Mobley, Identification of uropathogenic *Escherichia coli* surface proteins by shotgun proteomics, J. Microbiol. Methods 78 (2009) 131–135.
[51] C.J. Alteri, H.L. Mobley, Quantitative profile of the uropathogenic *Escherichia coli* outer membrane proteome during growth in human urine, Infect. Immun. 75 (2007) 2679–2688.
[52] G. Flatau, E. Lemichez, M. Gauthier, P. Chardin, S. Paris, C. Fiorentini, et al., Toxin-induced activation of the G protein p21 Rho by deamidation of glutamine, Nature 387 (1997) 729–733.
[53] P. Uhlen, A. Laestadius, T. Jahnukainen, T. Soderblom, F. Backhed, G. Celsi, et al., Alpha-haemolysin of uropathogenic *E. coli* induces Ca^{2+} oscillations in renal epithelial cells, Nature 405 (2000) 694–697.
[54] A. Doye, A. Mettouchi, G. Bossis, R. Clement, C. Buisson-Touati, G. Flatau, et al., CNF1 exploits the ubiquitin–proteasome machinery to restrict Rho GTPase activation for bacterial host cell invasion, Cell 111 (2002) 553–564.
[55] J.M. Davis, H.M. Carvalho, S.B. Rasmussen, A.D. O'Brien, Cytotoxic necrotizing factor type 1 delivered by outer membrane vesicles of uropathogenic *Escherichia coli* attenuates polymorphonuclear leukocyte antimicrobial activity and chemotaxis, Infect. Immun. 74 (2006) 4401–4408.
[56] C. Balsalobre, J.M. Silvan, S. Berglund, Y. Mizunoe, B.E. Uhlin, S.N. Wai, Release of the type I secreted alpha-haemolysin via outer membrane vesicles from *Escherichia coli*, Mol. Microbiol. 59 (2006) 99–112.
[57] M.C. Lane, C.J. Alteri, S.N. Smith, H.L. Mobley, Expression of flagella is coincident with uropathogenic *Escherichia coli* ascension to the upper urinary tract, Proc. Natl. Acad. Sci. U. S. A. 104 (2007) 16669–16674.
[58] C.K. Cusumano, C.S. Hung, S.L. Chen, S.J. Hultgren, Virulence plasmid harbored by uropathogenic *Escherichia coli* functions in acute stages of pathogenesis, Infect. Immun. 78 (2010) 1457–1467.
[59] W.J. Liang, K.J. Wilson, H. Xie, J. Knol, S. Suzuki, N.G. Rutherford, et al., The gusBC genes of *Escherichia coli* encode a glucuronide transport system, J. Bacteriol. 187 (2005) 2377–2385.
[60] D.G. Moriel, I. Bertoldi, A. Spagnuolo, S. Marchi, R. Rosini, B. Nesta, et al., Identification of protective and broadly conserved vaccine antigens from the genome of extraintestinal pathogenic *Escherichia coli*, Proc. Natl. Acad. Sci. U. S. A. 107 (2010) 9072–9077.
[61] D.L. Baldi, E.E. Higginson, D.M. Hocking, J. Praszkier, R. Cavaliere, C.E. James, et al., The type II secretion system and its ubiquitous lipoprotein substrate, SslE, are required for biofilm formation and virulence of enteropathogenic *Escherichia coli*, Infect. Immun. 80 (2012) 2042–2052.
[62] B. Nesta, M. Valeri, A. Spagnuolo, R. Rosini, M. Mora, P. Donato, et al., SslE elicits functional antibodies that impair in vitro mucinase activity and in vivo colonization by both intestinal and extraintestinal *Escherichia coli* strains, PLoS Pathog. 10 (2014), e1004124.
[63] U. Srinivasan, B. Foxman, C.F. Marrs, Identification of a gene encoding heat-resistant agglutinin in *Escherichia coli* as a putative virulence factor in urinary tract infection, J. Clin. Microbiol. 41 (2003) 285–289.
[64] R.P. Fagan, S.G. Smith, The Hek outer membrane protein of *Escherichia coli* is an auto-aggregating adhesin and invasin, FEMS Microbiol. Lett. 269 (2007) 248–255.
[65] G.C. Ulett, J. Valle, C. Beloin, O. Sherlock, J.M. Ghigo, M.A. Schembri, Functional analysis of antigen 43 in uropathogenic *Escherichia coli* reveals a role in long-term persistence in the urinary tract, Infect. Immun. 75 (2007) 3233–3244.
[66] N.J. Holden, B.E. Uhlin, D.L. Gally, PapB paralogues and their effect on the phase variation of type 1 fimbriae in *Escherichia coli*, Mol. Microbiol. 42 (2001) 319–330.
[67] Y. Xia, D. Gally, K. Forsman-Semb, B.E. Uhlin, Regulatory cross-talk between adhesin operons in *Escherichia coli*: inhibition of type 1 fimbriae expression by the PapB protein, EMBO J. 19 (2000) 1450–1457.
[68] N.J. Holden, D.L. Gally, Switches, cross-talk and memory in *Escherichia coli* adherence, J. Med. Microbiol. 53 (2004) 585–593.
[69] R.A. Hull, D.C. Rudy, W.H. Donovan, I.E. Wieser, C. Stewart, R.O. Darouiche, Virulence properties of *Escherichia coli* 83972, a prototype strain associated with asymptomatic bacteriuria, Infect. Immun. 67 (1999) 429–432.
[70] M. Hadjifrangiskou, M. Kostakioti, S.L. Chen, J.P. Henderson, S.E. Greene, S.J. Hultgren, A central metabolic circuit controlled by QseC in pathogenic *Escherichia coli*, Mol. Microbiol. 80 (2011) 1516–1529.
[71] S.E. Greene, J.S. Pinkner, E. Chorell, K.W. Dodson, C.L. Shaffer, M.S. Conover, et al., Pilicide ec240 disrupts virulence circuits in uropathogenic *Escherichia coli*, MBio. 5 (2014), e02038.
[72] M. Sabate, E. Moreno, T. Perez, A. Andreu, G. Prats, Pathogenicity island markers in commensal and uropathogenic *Escherichia coli* isolates, Clin. Microbiol. Infect. 12 (2006) 880–886.
[73] S.K. Wray, S.I. Hull, R.G. Cook, J. Barrish, R.A. Hull, Identification and characterization of a uroepithelial cell adhesin from a uropathogenic isolate of *Proteus mirabilis*, Infect. Immun. 54 (1986) 43–49.
[74] R. Pellegrino, P. Scavone, A. Umpierrez, D.J. Maskell, P. Zunino, *Proteus mirabilis* uroepithelial cell adhesin (UCA) fimbria plays a role in the colonization of the urinary tract, Pathog Dis. 67 (2013) 104–107.
[75] O. Sherlock, M.A. Schembri, A. Reisner, P. Klemm, Novel roles for the AIDA adhesin from diarrheagenic *Escherichia coli*: cell aggregation and biofilm formation, J. Bacteriol. 186 (2004) 8058–8065.
[76] E. Martinez, B. Bartolome, F. de la Cruz, pACYC184-derived cloning vectors containing the multiple cloning site and lacZ alpha reporter gene of pUC8/9 and pUC18/19 plasmids, Gene 68 (1988) 159–162.
[77] C.L. Ong, S.A. Beatson, A.G. McEwan, M.A. Schembri, Conjugative plasmid transfer and adhesion dynamics in an *Escherichia coli* biofilm, Appl. Environ. Microbiol. 75 (2009) 6783–6791.
[78] M. Ashburner, C.A. Ball, J.A. Blake, D. Botstein, H. Butler, J.M. Cherry, et al., Gene ontology: tool for the unification of biology, The Gene Ontology Consortium. Nat Genet., 25 2000, pp. 25–29.